Directional change in multivariable LQG control with actuator failure

D. HORLA*

Faculty of Electrical Engineering, Poznan University of Technology, 3A Piotrowo St., 60-965 Poznan, Poland

Abstract. The paper presents the phenomenon of directional change in LQG control of multivariable systems with amplitude constraints, as well as the impact of the latter on control performance. The interplay of directional change of the computed control vector with control performance has been thoroughly investigated, and is a result of the presence of constraints imposed on the applied control vector for different proportions of the number of control inputs to plant outputs. The impact of directional change phenomenon on the control performance has been defined, stating that performance deterioration is not tightly coupled with preservation of direction of the computed control vector. The statement has been supported by numerous simulation results for different types of plants with different LQG controller parameters.

Key words: directional change, actuator failure, windup phenomenon.

1. Introduction

The problem of robust control and stabilization is well-established in the literature. Some papers are related to performance measures in the quadratic cost sense for uncertain systems, as in [1] or [2], in the case of continuous-time control systems. In the case of discrete-time control systems, the guaranteed-cost control has been addressed in, e.g., [3].

In real-world applications actuators are prone to failures, thus it is of value to use the controller that can tolerate such situations, to guarantee stability and certain performance level. The paper adopts the approach presented in [4] in order to study the interplay between a special kind of actuator failure and phenomenon that takes place in multivariable control systems only, namely directional change.

This kind of actuator failure is a possible saturation of the elements of control vector, changing the information at the same time that is carried by the unconstrained (i.e., computed) control vector visible as directional change in controls. The state-feedback control law is proposed to guarantee the cost in the case of actuator failure, with failures modeled by scaling factors, that are used to project the „robustness area" on the static characteristic of the nonlinearity (saturation function) present in the control system.

A vast majority of real-world systems are subject to saturation-like actuator constraints or sensors' saturations. Such nonlinearities have negative impact on the control performance, and actuator saturation gives rise to windup phenomenon (lack of consistency between computed and constrained control input). The stability analysis results of saturated control systems may be found in, e.g. [5, 6].

Since unexpected actuator failures may cause severe damage, performance deterioration or might even be hazardous to the environment, it is of practical importance to analyze the interplay of control performance and directional change.

Independently of the kind of actuator failure, directional change modifies the proportions between the elements of the control vector. This aspect is usually omitted in the papers concerning windup phenomenon, and can be hardly ever seen in the works concerning multivariable systems. On the contrary to the SISO case, in the MIMO control systems one has to take cross-coupling and unequal number of plant inputs and outputs into consideration. The direction of computed control vector might not only fall in the principal input direction [7, 8] or can be related to maximal directional gain [9], but it can also reflect the degree of decoupling. Changing the control direction in such a case might cause performance deterioration.

Initial study of directional change in LQR control scheme has been presented in the previous work [10], though in the case of a square system only. This paper extends the results to non-square systems with perfect measurements, giving two conjectures that are supported by research carried out in [11] (improvement caused by introduction of no directional change in the case of one-input, six-outputs system) or [12] (with discussion of directional change impact on control quality for a set of controllers).

The main contribution of the paper is the identification of the interplay between directional change phenomenon, overall performance of the control system and dimensionality of the considered models. As a result, it would be possible to predict performance improvement/degradation when direction-preserving algorithm is implemented for non-square plant models in the case of robustness feature introduced to the control system. It has to be stressed that the presented design criteria of the LQG controller do not take dimension of the plant explicitly, but by observing performance indices' values it is possible to identify where it is advantageous to apply the proposed approach.

---
*e-mail: dariusz.horla@put.poznan.pl

2. Plant and actuator failure models

The following multivariable model is taken into consideration:

$$\underline{x}_{t+1} = A\underline{x}_t + B\underline{u}_t + \underline{\xi}_t, \tag{1}$$

$$\underline{y}_t = C\underline{x}_t, \tag{2}$$

with $\underline{\xi}_t$ as vector disturbance with covariance matrix $\sum_\xi = \{\sigma_\xi^2, \sigma_\xi^2, \ldots, \sigma_\xi^2\}$, statistically independent with zero mean value, with the possibility of perfect measurements [13]. The output vector $\underline{y} \in \mathscr{R}^p$, the constrained control vector $\underline{u} \in \mathscr{R}^m$ (on the contrary to the computed control vector $\underline{v} \in \mathscr{R}^m$, and the state vector $\underline{x} \in \mathscr{R}^n$.

The control performance index is defined as

$$J = E\left\{\sum_{t=0}^{\infty} \left(\underline{x}_t^T Q\underline{x}_t + \underline{u}_t^T R\underline{u}_t\right)\right\}, \tag{3}$$

with weighing matrices $Q \geq 0$, $R \geq 0$. Taking possible saturations into account, one can assume actuator failure model as in [18], i.e.,

$$\begin{aligned} u_{t,i}^k &= (1 - \rho_{t,i}^k)\mathrm{sat}(v_{t,i}; \alpha_i) \\ &(i = 1, 2, \ldots, m, \quad k = 1, 2, \ldots, g), \end{aligned} \tag{4}$$

where $\rho_{t,i}^k$ is an unknown constant from the span that will be defined in the further part of the text, index k denotes the k-th failure model, and g is the total number of failure models. The notation $u_{t,i}^k$ corresponds to the i-th component of the constrained control vector, assuming that an actuator failure takes place (in the other case, $u_{t,i}^k = v_{t,i}$). For any actuator failure model, including the situation for constraints imposed on the control vector, the constant $\rho_{t,i}^k$ lies in $\rho_{-,t,i}^k \leq \rho_{t,i}^k \leq \rho_{+,t,i}^k$, and function sat defines the method od applying constraints (e.g., cut-off constraint).

The control vector might be either constrained by a cut-off nonlinearity, changing its direction in general, what can be treated as an actuator failure case, or by direction-preserving (DP) saturation algorithm. The latter is the core of this paper.

If $\rho_{-,t,i}^k = \rho_{+,t,i}^k = 0$ holds in (4), it means that failure (4) has not taken place (there is only the saturation of the i-th control signal present). If $\rho_{-,t,i}^k = \rho_{+,t,i}^k = 1$ holds, it corresponds to outage case in the k-th failure model. The failure according to the k-th model means that $0 < \rho_{-,t,i}^k \leq \rho_{+,t,i}^k < 1$ holds.

In the most general case, having taken a single model of failure into account, i.e. $u_{t,i}^F = u_{t,i}^k$, (4) can be transformed [4, 13, 14], to

$$u_{t,i}^F = \rho_i v_{t,i} \quad (i = 1, 2, \ldots, m), \tag{5}$$

where ($\rho_{-,i} \leq 1$ and $\rho_{+,i} \geq 1$)

$$0 \leq \rho_{-,i} \leq \rho_i \leq \rho_{+,i} \quad (i = 1, 2, \ldots, m). \tag{6}$$

In analogy to (4), $\rho_{-,i} = \rho_{+,i}$ for $i = 1, \ldots, m$ means that there are no active constraints imposed on the control vector, and $u_{t,i}^F = u_{t,i}$ (i.e. linear range of controller's actions). The case $\rho_{-,i} > 0$ corresponds to partial failure, and $\rho_{-,i} = 0$ to the outage case, as mentioned earlier. This is a more general case in comparison with (4), since relation between computed and applied control signals is taken into account.

In order to streamline the further presentation, the following notation has been adopted from [13, 14]:

$$\underline{u}_t^T = \left[u_{t,1}^F, u_{t,2}^F, \ldots, u_{t,m}^F\right]^T, \tag{7}$$

$$\rho_+ = \mathrm{diag}\{\rho_{+,1}, \rho_{+,2}, \ldots, \rho_{+,m}\}, \tag{8}$$

$$\rho_- = \mathrm{diag}\{\rho_{-,1}, \rho_{-,2}, \ldots, \rho_{-,m}\}, \tag{9}$$

$$\rho = \mathrm{diag}\{\rho_1, \rho_2, \ldots, \rho_m\}. \tag{10}$$

3. Directional change phenomenon

Depending on the method of imposing constraints on the control vector, one can observe directional change, illustrated in Fig. 1a in the case of cut-off saturation, which is not present when saturation is performed according to the imposed constraints (dashed lines) with constant direction, Fig. 1b.
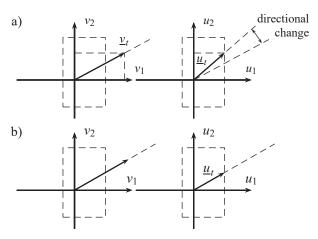

Fig. 1. a) direction-changing, b) direction-preserving saturation (left: control vector before amplitude saturation, right: after saturation)

4. Control law

The control law of the form

$$\underline{v}_t = F\underline{x}_t \tag{11}$$

is called reliable, i.e.,assuring that a specified value of the performance index (3) is not exceeded, if it is connected to a ceratin matrix P that satisfies the inequality [13, 14]

$$(A + B\rho F)^T P(A + B\rho F) - P + F^T \rho R\rho F + Q \leq 0. \tag{12}$$

The closed loop system

$$\underline{x}_{t+1} = (A + B\rho F)\underline{x}_t \tag{13}$$

is then stable, and the performance index in an infinite horizon satisfies

$$J = E\left\{ \sum_{t=0}^{\infty} \underline{x}_t^T \left(Q + F^T \rho R \rho F \right) \underline{x}_t \right\} \leq \tag{14}$$
$$\leq \underline{x}_0^T P \underline{x}_0 + \text{trace}\left(P \Sigma_\xi \right).$$

If no robustness against actuator failure is taken into consideration, the optimal state-feedback matrix $F°$ for the control law (11) is derived as a solution of the set of equations [14]:

$$F° = -\left(B^T P° B + R \right)^{-1} B^T P° A, \tag{15}$$

$$P° = Q + A^T P° A - A^T P° B \left(B^T P° B + R \right)^{-1} B^T P° A, \tag{16}$$

and the optimal value $J_{F°}$ of (3), based on deriving $F°$ according to (15) and (16) being at the same time the upper boundary of (14) in the case of no actuator failure, is

$$J_{F°} = \underline{x}_0^T P° \underline{x}_0 + \text{trace}\left(P° \Sigma_\xi \right). \tag{17}$$

5. Derivation of optimal state-feedback matrix in the case of actuator failure

The case of cut-off and direction-preserving saturation functions are considered below, in which case one can give the following algorithm [13, 14] enabling derivation of the optimal state-feedback matrix F to increase the robustness of the system against actuator failure:

1) solve (16) with respect to P (mark the result as P^*), and choose an arbitrary diagonal matrix R_0, satisfying

$$R_0 \leq \left(B^T P^* B + R \right)^{-1}; \tag{18}$$

2) solve

$$P = Q + A^T P A - A^T P J_0 P A \tag{19}$$

with respect to the stabilizing P and check the condition

$$R_0 \leq \left(B^T P B + R \right)^{-1}, \tag{20}$$

where

$$J_0 = B \left(I - \Gamma_0^2 \right) \left(\left(B^T P B + R \right) \left(I - \Gamma_0^2 \right) + \right.$$
$$\left. + R_0^{-1} \Gamma_0^2 \right)^{-1} B^T, \tag{21}$$

(matrix Γ_0 will be defined in due course of the paper);
3) if the inequality (18) is satisfied for R_0 and P, increase the elements of R_0 and proceed to step 2; otherwise, decrease

the elements of R_0 and proceed to step 2, checking if step 4 is satisfied;

4) if the inequality (18) is satisfied for R_0 and P, the stabilizing matrix P satisfies the equation (19), and there is no positive-definite solution for the pair R_0 and P for arbitrary R_0', where $R_0 \leq R_0' \leq (B^T P^* P + R)^{-1}$, then stop the algorithm; in this case, the state-feedback matrix is given as

$$F = -\Gamma^{-1}\left(I - \left(X^{-1} - R_0 \right) \left(\left(I - \Gamma_0^2 \right) + \right. \right.$$
$$\left. \left. + \Gamma_0^2 R_0^{-1} X^{-1} \right)^{-1} \Gamma_0^2 R_0^{-1} \right) X^{-1} B^T P A, \tag{22}$$

where $X = B^T P B + R$.

The following notation has been adopted in the considered algorithm [13]:

$$\Gamma = \text{diag}\left\{ \gamma_1, \gamma_2, \ldots, \gamma_m \right\}, \tag{23}$$

$$\Gamma_0 = \text{diag}\left\{ \gamma_{0,1}, \gamma_{0,2}, \ldots, \gamma_{0,m} \right\}, \tag{24}$$

where:

$$\gamma_i = \frac{\rho_{+,i} + \rho_{-,i}}{2}, \tag{25}$$

$$\gamma_{0,i} = \frac{\rho_{+,i} - \rho_{-,i}}{\rho_{+,i} + \rho_{-,i}}. \tag{26}$$

The matrix P satisfying the equation

$$P = Q + A^T P A - A^T P B \left(B^T P B + R \right)^{-1} B^T P A \tag{27}$$

is called the stabilizing solution to the Ricatti equation, and all eigenvalues of the matrix $A - B(B^T P B + R)^{-1} B^T P A$ are inside the unit circle.

In addition, on the basis of (10, 23 and 24) we have [4]:

$$\rho = (I + \rho_0)\Gamma, \tag{28}$$

$$|\rho_0| \leq \Gamma_0 \leq I, \tag{29}$$

where matrix $\rho_0 = \text{diag}\{\rho_{0,1}, \rho_{0,2}, \ldots, \rho_{0,m}\}$, $\rho_{0,i} = \frac{\rho_i - \gamma_i}{\gamma_i}$ ($i = 1, \ldots, m$), and operation of the absolute value $|\rho_0|$ is elementalism for the whole matrix.

6. Actuator failure and control subject to constraints

Amplitude-constrained control, where the input signals of the actuator can saturate, may be treated as a special case of the actuator failure, thus one can model possible saturations of the control signals as a case of actuator failures (for successful application to a real-world process, see e.g. [15]). In such a situation, it is assumed that $\gamma_i = \alpha_i$ for $i = 1, 2, \ldots, m$, and i-th component of the constrained control vector becomes [14]
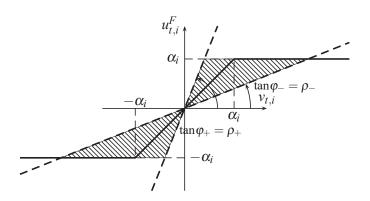
Fig. 2. Actuator failure and amplitude constraints

$$u^F_{i,t} = \text{sat}\left(\underline{f}^T_i \underline{x}_t; \alpha_i\right), \tag{30}$$

where sat is a function that imposes constraints on the i-th component of control vector in the span of $\pm\alpha_i$, and $\underline{f}^T_i$ is the i-th row of F. With reference to comments in Section 2, and (5), $\rho_i = 1$ holds whenever the i-th component of the control vector is in a linear range, and $\rho_i \neq 1$ otherwise. In other words, actuator failure in (30) refers to discrepancy between computed and applied control signals, as in (4, 5).

An isolated actuator failure on the basis of (5) and (30) is presented in the Fig. 2. The assumed failure model can be put for the complete system in the form ($i = 1, 2, \ldots, m$)

$$u^F_{i,t} = \text{sat}\left(\rho_i v_{t,i}; \alpha_i\right), \tag{31}$$

as a compilation of models (30) and (5) (dashed area in Fig. 2).

The situation from the Fig. 2 can be extended to the case of simultaneous amplitude and rate constraints having assumed that the domain of acceptable solutions is non-empty and it includes the area of guaranteed performance index value. Should the domain be empty, the rate constraints are treated as secondary and thus omitted.

7. Simulation results

7.1. Model parameters.
The following models are taken into consideration (in all the cases $C = [I, 0]$ with appropriate dimensions of the inner matrices):

• P1 ($m = 2$, $p = 2$)

$$A = \left[\begin{array}{cc|c} -0.80 & 0.10 & I \\ -0.40 & 1.00 & \\ \hline 0.49 & 0.10 & 0 \\ -0.10 & -0.25 & \end{array}\right],$$

$$B = \left[\begin{array}{cc} 1.0 & 0.3 \\ 0.5 & 0.8 \\ 0.0 & 0.0 \\ 0.0 & 0.0 \end{array}\right],$$

• P2 ($m = 3$, $p = 2$)

$$A = \left[\begin{array}{cc|c} -0.80 & 0.10 & I \\ -0.40 & 1.00 & \\ \hline 0.49 & 0.10 & 0 \\ -0.10 & -0.25 & \end{array}\right],$$

$$B = \left[\begin{array}{ccc} 1.0 & 0.2 & 0.3 \\ 0.5 & 0.3 & 0.8 \\ 0.0 & 0.0 & 0.0 \\ 0.0 & 0.0 & 0.0 \end{array}\right],$$

• P3 ($m = 2$, $p = 3$)

$$A = \left[\begin{array}{ccc|c} 0.7 & 0.0 & -0.1 & I \\ 0.1 & 0.8 & -0.2 & \\ -0.1 & 0.0 & 0.8 & \\ \hline 0.1 & 0.0 & 0.0 & 0 \\ 0.0 & -0.1 & 0.0 & \\ 0.0 & 0.0 & -0.5 & \end{array}\right],$$

$$B = \left[\begin{array}{cc} 1.0 & 0.1 \\ 0.2 & 1.0 \\ 0.5 & -0.1 \\ 0.0 & 0.0 \\ 0.0 & 0.0 \\ 0.0 & 0.0 \end{array}\right],$$

in order to cover the cases with $m = p$, $m > p$, $m < p$.

7.2. Figures and tables.
7.2.1. Preliminaries.
A set of simulations has been performed in the horizon of $N = 10\,000$ steps, assuming that the state vector is to be stabilized at the origin subject to constraints acting on it, with disturbance variances equal to 0.1; the initial results have been described in [14] (carried out for the same plant models described as P1, P2, P3).

The tests have been performed assuming that there is a symmetrical cut-off amplitude saturation in the system, identical for all m control inputs, for the fixed values of α and variable δ and for fixed values of δ and variable α. In addition, it has been assumed that $\rho_+ = 1 + \delta$, $\rho_- = 1 - \delta$, and the performance index J is computed as an expected value.

In order to verify the behavior of the control system, two additional performance indices have been introduced, related to mean absolute and squared tracking errors. Here $\underline{r}$ denotes a square-wave reference vector tracked by output plant vector. Tracking property is due to introducing an the offset/shift to the control vector (11) related to the current values of the reference vector, allowing its asymptotic tracking. As a result, the control vector is a sum of (11) and offset vector, what results in y being shifted accordingly to the values in $\underline{r}$. In the case of $m \leq p$ there are two square waves in reference vector delayed by half of the period as a reference vector, with amplitudes ± 3 and period of

40 samples, whereas in the case of $m > p$ the third reference signal is zero. The indices are:

$$J_1 = \frac{1}{N} \sum_{t=0}^{N} \sum_{k=1}^{p} |r_{k,t} - y_{k,t}|, \tag{32}$$

$$J_2 = \frac{1}{N} \sum_{t=0}^{N} \sum_{k=1}^{p} (r_{k,t} - y_{k,t})^2, \tag{33}$$

where N denotes the simulation horizon.

In order to evaluate the directional change impact on the control performance, the following indices are introduced:

$$J_\varphi = \frac{1}{N} \sum_{t=0}^{N} |\varphi(\underline{v}_t) - \varphi(\underline{u}_t)| \; [°], \tag{34}$$

$$J_{\varphi^2} = \frac{1}{N} \sum_{t=0}^{N} \left(\varphi(\underline{v}_t) - \varphi(\underline{u}_t) \right)^2, \tag{35}$$

where $\varphi(\underline{v}_t)$ is an angle between $\underline{e}_1$ and $\underline{v}_t$, and $\varphi(\underline{u}_t)$ is an angle between $\underline{e}_1$ and $\underline{u}_t$.

Index J_φ is related to the mean absolute directional change (in degrees), and its value increases in proportion to the excess of the directional change. Performance index J_{φ^2} increases rapidly with severe directional change, and allows one to check what is the character of these changes.

7.2.2. Index J (3) vs. amplitude constraint α. Based on Fig. 3, one can state that by increasing the area of robust perfor-

mance (i.e., by increasing δ) we can observe a local minimum of the performance index for tough constraints. On the basis of Fig. 3a, one can say that the control system is stable from $\alpha = 0.6$, $J = 0.2551$ ($\delta = 0.3$), $\alpha = 0.5$, $J = 0.3142$ ($\delta = 0.7$) up to $\alpha = 0.4$, $J = 0.4438$ ($\delta = 0.8$). There is a decrease of the performance index at $\delta = 0.8$ visible in the Figures for the case of P1 and P2 and tightening constraints.

The plots of J for the toughest constraints start at:
- P1: 0.4438\$ for $\delta = 0.8$, 0.3142 for $\delta = 0.7$,
- P1-DP: 0.4158 for $\delta = 0.8$, 0.3088 for $\delta = 0.7$,
- P2: 0.4367\$ for $\delta = 0.8$, 0.3338 for $\delta = 0.7$,
- P2-DP: 0.4344 for $\delta = 0.8$, 0.3297 for $\delta = 0.7$,

and end (in order) at: 0.4312 for $\delta = 0.8$ and 0.3028 for $\delta = 0.7$ (both for P1) as well as 0.4487 for $\delta = 0.8$ and 0.3136 for $\delta = 0.7$ (both for P2).

The plant P3 is the opposite case: the decrease of the performance index takes place in the whole range of δ (from 0.1 to 0.8), and the performance index J decreases for the system without constraints with the increase in δ.

It can be stated that when the controller is static, one can improve the performance when DP algorithm is considered with respect to a cut-off saturation, in the sense that the performance index decreases when control vector saturates (see Fig. 3a and b), enabling at the same time the system to operate in stable mode with tougher values of α and by decreasing the values of the performance index for large δ and tougher constraints. In the case of P2 model, this is connected with $m > p$.

In the case of P3, when there is no directional change allowed, the index J degrades at non-impending values of α, what is connected to the deficient number of control signals with respect to plant outputs. The plots of J_1 end at:

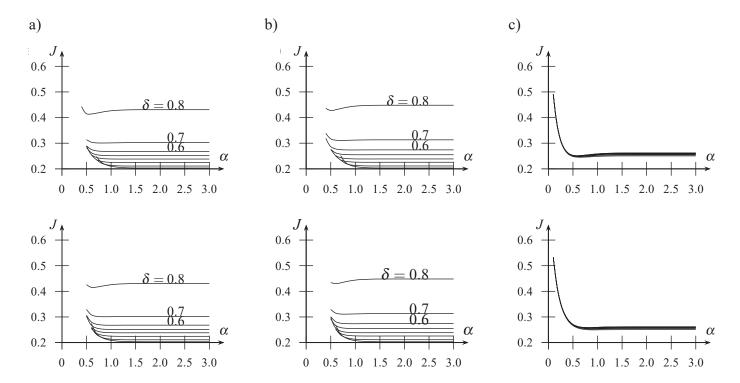a)   b)   c)

Fig. 3. Performance index J against α (upper row: cut-off, lower row: DP constraint), a) P1, b) P2, c) P3

- P1 (both): 0.7234 for $\delta = 0.8$, 0.6144 for $\delta = 0.7$,
- P2 (both): 0.7358 for $\delta = 0.8$, 0.6242 for $\delta = 0.7$,

and the plots of J_2 at:

- P1 (both): 0.4313 for $\delta = 0.8$, 0.3028 for $\delta = 0.7$,
- P2 (both): 0.4487 for $\delta = 0.8$, 0.3137 for $\delta = 0.7$.

In the case of P3, the plots for different values of δ are alike for each of the performance indices either for the non-DP or DP system. Introducing the DP requirement increases performance indices. This is on the contrary to the case of dynamical controllers, see [16].

7.2.3. J_1 i J_2 indices vs. amplitude constraint α. On the basis of Figs. 4 and 5, one can formulate similar conclusions concerning indices J_1, J_2 and J, as previously. It is, however, interesting that control system with P3 is stable even for tough constraints α, i.e. from 0.1 in the given robustness area.
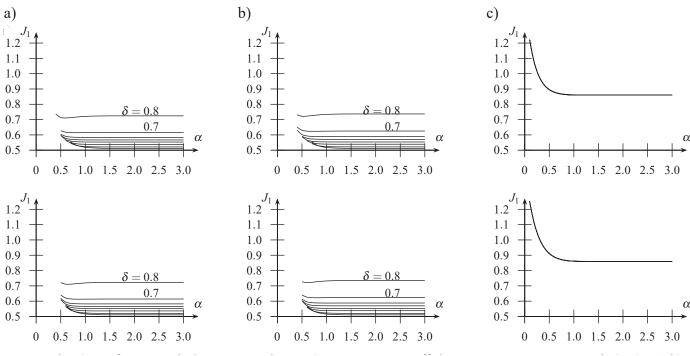

Fig. 4. Performance index J_1 against α (upper row: cut-off, lower row: DP constraint), a) P1, b) P2, c) P3
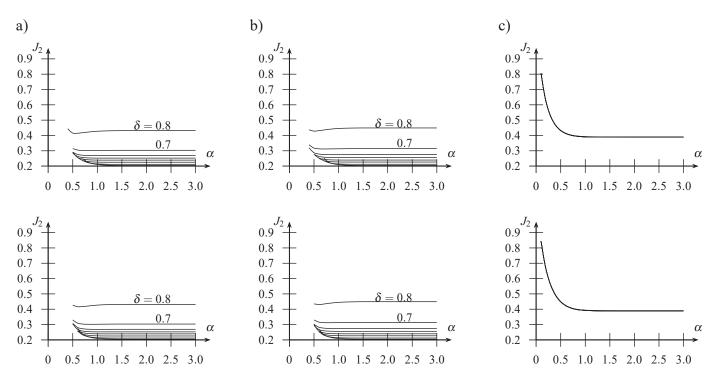

Fig. 5. Performance index J_2 against α (upper row: cut-off, lower row: DP constraint), a) P1, b) P2, c) P3

7.2.4. J, J_1 and J_2 indices vs. amplitude constraint δ. On the basis of Fig. 6, plots of the characteristics start at:
- P1: 0.2738 for $\alpha = 0.55$, 0.2488 for $\alpha = 0.70$,
- P1-DP: 0.2892 for $\alpha = 0.55$, 0.2365 for $\alpha = 0.70$,
- P2: 0.3232 for $\alpha = 0.40$, 0.2711 for $\alpha = 0.55$, 0.2525 for $\alpha = 0.70$,
- P2-DP: n/a for $\alpha = 0.40$, 0.2791 for $\alpha = 0.55$, 0.2336 for $\alpha = 0.70$,

- P3: 0.4921 for $\alpha = 0.10$, 0.3127 for $\alpha = 0.25$, 0.2622 for $\alpha = 0.40$,
- P3-DP: 0.5325 for $\alpha = 0.10$, 0.3528 for $\alpha = 0.25$, 0.2844 for $\alpha = 0.40$.

The plots depicted in Fig. 7 start at:
- P1: 0.5797 for $\alpha = 0.55$, 0.5544 for $\alpha = 0.70$,
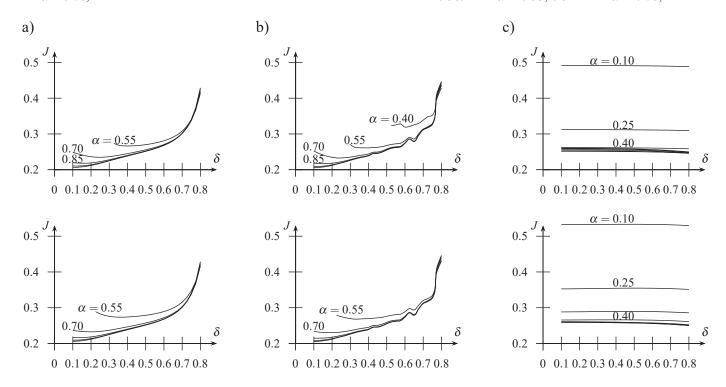- P1-DP: 0.5891 for $\alpha = 0.55$, 0.5444 for $\alpha = 0.70$,

Fig. 6. Performance index J against δ (upper row: cut-off, lower row: DP constraint), a) P1, b) P2, c) P3
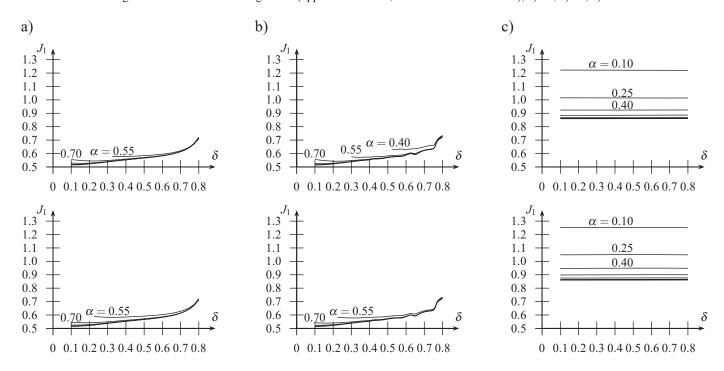

Fig. 7. Performance index J_1 against δ (upper row: cut-off, lower row: DP constraint), a) P1, b) P2, c) P3
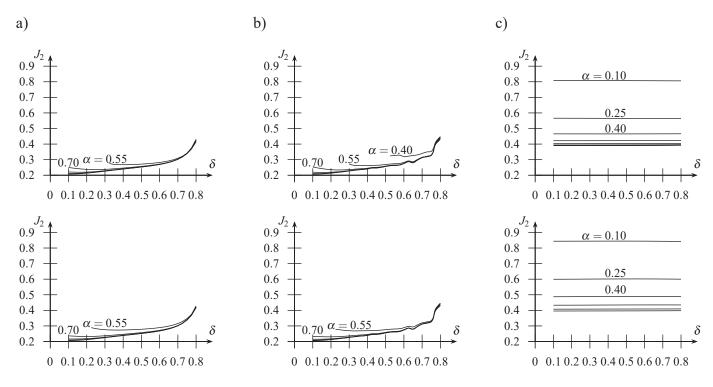
a)

b)

c)

Fig. 8. Performance index J_2 against δ (upper row: cut-off, lower row: DP constraint), a) P1, b) P2, c) P3

- P2: 0.6292 for $\alpha = 0.40$, 0.5762 for $\alpha = 0.55$, 0.5556 for $\alpha = 0.70$,
- P2-DP: n/a for $\alpha = 0.40$, 0.5817 for $\alpha = 0.55$, 0.5414 for $\alpha = 0.70$,
- P3: 1.2222 for $\alpha = 0.10$, 1.0112 for $\alpha = 0.25$, 0.9238 for $\alpha = 0.40$,
- P3-DP: 1.2525 for $\alpha = 0.10$, 1.0484 for $\alpha = 0.25$, 0.9474 for $\alpha = 0.40$.

The plots depicted in Fig. 8 start at:
- P1: 0.2738 $\alpha = 0.55$, 0.2489 for $\alpha = 0.70$,
- P1-DP: 0.2892 for $\alpha = 0.55$, 0.2366 for $\alpha = 0.70$,
- P2: 0.3233 for $\alpha = 0.40$, 0.2711 for $\alpha = 0.55$, 0.2525 for $\alpha = 0.70$,
- P2-DP: n/a for $\alpha = 0.40$, 0.2792 for $\alpha = 0.55$, 0.2336 for $\alpha = 0.70$,
- P3: 0.8073 for $\alpha = 0.10$, 0.5650 for $\alpha = 0.25$, 0.4646 for $\alpha = 0.40$,
- P3-DP: 0.8441 for $\alpha = 0.10$, 0.5999 for $\alpha = 0.25$, 0.4876 for $\alpha = 0.40$.

It is evident, though, that regardless of the type of the performance index for P1 and P2, introducing the DP requirement causes improvement of the indices. This is the case of a static controller, unable to perform correcting action over a series of steps. The decrease is visible for δ down to 0.4 for amplitude constraints less severe than $\alpha = 0.55$.

Because of the fact that $m < p$ in the case of P3, this phenomenon is not observed here. Changing the computed control vector direction in the case of this plant is mostly connected to the quality of decoupling by the controller.

In the case of P1 and P2, the listed indices for large δ tend approximately to the same values that increase to a very minor extent for tougher constraints.

7.3. Directional change in controls. The plots of performance indices have been presented in Figs. 9 and 10 for variable α (upper part) and δ (lower part). On the basis of the plots for variable δ and plants P1 and P2, one can see that for every constraint value considered there is such a specific value of δ corresponding to the volume of the robustness area that directional change between computed and constrained control vectors is minimal. As an example, for P1 and $\alpha = 0.55$ we have the minimum at $\delta = 0.42$, for $\alpha = 0.70$ at $\delta = 0.40$ and for $\alpha = 0.85$ at $\delta = 0.39$. In this case, minimal directional change corresponds to increasing the robustness area.

Having assumed that for P2 and $\alpha = 0.70$ with $\delta = 0.40$ we have the minimum, with corresponding $\rho_- = 1 - \delta = 0.6$, and one can draw a line on Fig. 2 at angle of $45° - 31° = 14°$ that intersects the line $u_{t,i}^F = 0.70$ at $v_{t,i} = 1.16$. It can be understood then that elements of control vector up to the amplitude of 1.16 lie inside the robustness area, what explains why the observed increase for the indices for $\delta > 0.4$ is not large for less tough constraints and why it increases for $\delta < 0.4$.

Increasing the robustness area for P3 and performance indices of J-type, does not cause the degradation in control performance (performance indices are approximately invariant), what is additionally verified for in the upper part of Figs. 9 and 10, showing virtually no change in the characteristics of the plots as a function of α for variable δ.

Fig. 9. Performance index J_φ against α (upper row), δ (lower row), a) P1, b) P2, c) P3

Fig. 10. Performance index J_{φ^2} against α (upper row), δ (lower row), a) P1, b) P2, c) P3

On the basis of Figs. 9a and b, as well as Figs. 10a and b, one can see that for P1 and P2 with less severe constraints one can observe an initial increase in directional change, and with further less impending constraints, decrease in directional change, i.e. decrease of the performance indices measuring angular change.

8. Conjectures – summary

As it has been presented in the paper, the increase in control performance indices does not have to be connected with the increase in intensity of directional change. By introducing the degree of robustness against the actuator failure corresponding

to, e.g., cut-off or DP constraint, there is a possibility of further performance index reduction what is related to better anti-windup compensation with simultaneous minimal directional change possible.

Conjecture 1. By increasing the robustness area for controllable plants with cut-off saturation and $m \geq p$ performance indices increase. For tougher constraints performance indices initially decrease, to increase in the end. In such a case, introducing the DP constraint improves their values, assuring faster desaturation of the control vector.

Conjecture 2. In the considered control system, for controllable plants with $m < p$ introduction of DP constraint causes performance indices to increase. In this case, there is no reason to implement the controllers with DP algorithm.

REFERENCES

[1] S.S.L. Chang and T.K.C. Peng, "Adaptive guaranteed cost control of systems with uncertain parameters", IEEE Transactions on Automatic Control 17 (4), 474–483 (1972).

[2] I.R. Petersen and D.C. McFarlane, "Optimizing the guaranteed cost in the control of uncertain systems", in *Robustness of Dynamical Systems with Parameter Uncertainties*, eds. M. Mansour, S. Balemi, and W. Truol, Brikhäuser, Boston, 1992.

[3] L. Xie and Y.C. Soh, "Guaranteed cost control of uncertain discrete-time systems", *Control Theory and Advanced Technology* 10, 1235–1251 (1995).

[4] Y. Yang, G.-H. Yang, and Y.C. Soh, "Reliable control of discrete-time systems with actuator failures", *IEE Proceedings – Control Theory and Applications* 147 (4), 428–432 (2000).

[5] T. Hu and Z. Lin, *Control Systems with Actuator Saturation: Analysis and Design*, Birkhäuser, Boston, 2001.

[6] S. Tarbouriech and J. Gomes da Silva, "Synthesis of controllers for continuous-time delay systems with saturating controls via LMIs", *IEEE Transactions on Automatic Control* 45 (1), 105–111 (2000).

[7] J.M. Maciejowski, *Multivariable Feedback Design*, Addison-Wesley Publishing Company, Cambridge, 1989.

[8] J.M. Maciejowski, *Predictive Control with Constraints*, Pearson Education Limited, Harlow, 2002.

[9] P. Albertos and A. Sala, *Multivariable Control Systems*, Springer, London, 2002.

[10] D. Horla, "Directional change issues in LQG control with actuator failure", *Proceedings of the 7th IFAC Conference on Manufacturing Modelling, Management and Control MIM'2013*, 1810–1814 (2013).

[11] D. Horla, R. Lewandowski, A. Schmidt, M. Kraft, and W. Giernacki, "Active vibration reduction system optimal control using linear matrix inequalities with no directional change in controls", *Asian Journal of Control* 15 (6), 1571–1578 (2013).

[12] D. Horla, "On directional change and anti-windup compensation in multivariable control systems", *International Journal of Applied Mathematics and Computer Science* 19 (2), 281–289 (2009).

[13] G.-H. Yang, J.L. Wang, and Y.C. Soh, "Reliable LGQ control with sensor failures", *IEE Proceedings – Control Theory and Applications* 147 (4), 433–439 (2000).

[14] D. Horla and A. Królikowski, "Discrete-time LQG control with actuator failure", *Proceedings of the 8th International Conference on Informatics in Control, Automation and Robotics* 1, 517–521 (2011).

[15] A. Owczarkowski and D. Horla, "Robust LQR and LQI control with actuator failure of a 2DOF unmanned bicycle robot stabilized by an inertial wheel", *International Journal of Applied Mathematics and Computer Science* 26 (2), 325–334 2016.

[16] D. Horla, "Interplay of directional change in controls and windup phenomena. Analysis and synthesis of compensators", PhD thesis, Poznan University of Technology, Poznan 2012.